Spectrum and space resolved 4D imaging by coded aperture correlation holography (COACH) with diffractive objective lens

A. Vijayakumar* and Joseph Rosen

Department of Electrical and Computer Engineering, Ben-Gurion University of the Negev, P.O. Box 653, Beer-Sheva 8410501, Israel
Corresponding author: physics.vijay@gmail.com

In this Letter, we present an advanced optical configuration of coded aperture correlation holography (COACH) with a diffractive objective lens. Four-dimensional imaging of objects at the three spatial dimensions and with an additional spectral dimension is demonstrated. A hologram of three-dimensional objects illuminated by different wavelengths was recorded by the interference of light diffracted from the objects with the light diffracted from the same objects, but through a random-like coded phase mask (CPM). A library of holograms denoted point spread function (PSF) holograms were prerecorded with the same CPM, and under identical conditions, using point objects along different axial locations and for the different illuminating wavelengths. The correlation of the object hologram with the PSF hologram recorded using a particular wavelength, and at a particular axial location, reconstructs only the object corresponding to the particular axial plane and to the specific wavelength. The reconstruction results are compared with regular imaging and with another well-established holographic technique called Fresnel incoherent correlation holography. © 2017 Optical Society of America

Holography, invented by Dennis Gabor, revolutionized the field of imaging by introducing the possibility of recording and reconstructing three-dimensional (3D) spatial information of objects [1,2]. Digital holography, the modern technique of holography, has replaced regular imaging in numerous applications due to its various advantages [3–6]. Capturing, and storing on a hologram, information from additional dimensions beyond the well-known three spatial dimensions can be useful for various applications. Digital holographic techniques have been developed in the recent years for recording and reconstructing information beyond the three spatial dimensions [7–12].

A unique digital holographic technique termed Fresnel incoherent correlation holography (FINCH) using incoherent light was invented in 2007 [13,14]. FINCH is classified in the category of self-informative reference holography, in which the light diffracted by every point on the object under study is interfered with itself, and both interfering beams contain the information of the point location. This self-interference effect in FINCH has pushed its lateral resolution limits beyond the classical limits dictated by the Lagrange invariant law [15–19]. However, the axial resolution of FINCH was found to be lower than that of regular imaging. In this line of research, a useful incoherent self-referenced digital holographic system dubbed coded aperture correlation holography (COACH) has been developed most recently [20]. Due to the use of a random-like coded phase mask (CPM), instead of the quadratic phase mask of FINCH, the axial resolution has been improved [20]. COACH was found to possess axial and lateral resolutions similar to that of an equivalent regular imaging system but, unlike the last one, a single hologram of COACH has the capability of recording and reconstructing 3D scenes. One of the limitations of COACH was the inherent background noise generated during reconstruction. Different noise reduction techniques such as phase-only filtering, averaging and hybridization techniques were developed to minimize the background noise generated in COACH [21].

In this Letter, we present an advanced configuration of COACH for recording and reconstructing objects with spatial, as well as spectral information and, thus, the system demonstrates four-dimensional (4D) imaging. Recording and reconstructing the additional spectral information can be useful for hyperspectral imaging as well as for imaging spectrometer [22]. The high axial resolution of COACH arising from the relatively short axial correlation lengths of the random-like CPM is exploited to extend the information acquisition in order to resolve not only spatial, but also spectral information.

The optical configuration of 4D-COACH is shown in Fig. 1. The description is given for only two wavelengths, although it can be straightforwardly generalized for polychromatic light. The light from two incoherent sources of different wavelengths is focused to critically illuminate [23] two different axial planes of a multiplane object. The beams with two wavelengths λ_1 and λ_2 diffracted from different planes of the object are incident on a diffractive lens (DL) of focal length $f_{\lambda 1}$ mounted at a distance
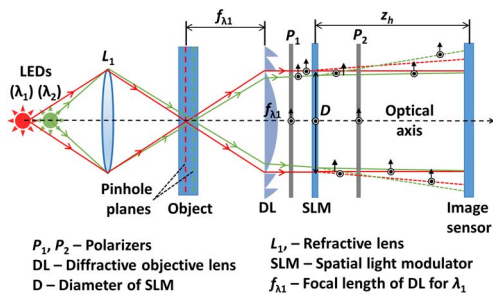
Fig. 1. COACH configuration for recording the object and PSF holograms.

Fig. 2. Normalized intensity of the reconstructed/imaged point at $\lambda = 633$ nm for different wavelengths for COACH, FINCH, and regular imaging with a refractive and diffractive objective lens.

$\sim f_{\lambda 1}$ from the object. The DL is sensitive to wavelengths and, thus, the focal distance of the DL is different for different wavelengths. Hence, even when both the wavelengths illuminate the same axial plane of the object, they are focused at different distances due to the dispersion of the DL. Since all sources are spatially incoherent, the light emitted by each object point with a specific wavelength is coherent only with itself and, therefore, can only interfere with itself. The beam diffracted by the DL is polarized by polarizer P_1 oriented at 45° with respect to the active axis of the spatial light modulator (SLM). Similar to [20], a random-like CPM, calculated using the Gerchberg–Saxton algorithm [24,25] to obtain uniform intensity in the spectrum domain, is displayed on the SLM. As the polarization of the collimated light is oriented at 45° with respect to the active axis of the SLM, only about half of the intensity of the incident light is modulated by the phase profile displayed on the SLM. The remaining half of the intensity passes through the SLM without any modulation. A second polarizer P_2 also oriented 45° with respect to the active axis of the SLM projects the modulated and the unmodulated components onto the same orientation such that the beams interfere on the sensor plane. This multiplexing scheme adapted from [26] allows the generation of two interfering beams in a compact single channel optical configuration. The twin image and the bias terms present in the hologram are cancelled out by a phase-shifting procedure involving recording of three holograms corresponding to the three phase values $\theta = 0°$, 120°, and 240° followed by their superposition [13]. A library of complex holograms dubbed PSF holograms $H_{PSF}(\lambda, z)$ is synthesized from three phase-shifting holograms. These PSF holograms are recorded by shifting a pinhole along all possible axial locations of objects and by illuminating the pinhole with entire wavelengths used in the setup. The library $H_{PSF}(\lambda, z)$ is prepared once and is later used for any number of times for reconstructing the entire object holograms. Once the library is ready for use, the pinholes are replaced by objects, and complex holograms of the 3D objects, named H_{object}, are recorded by the same phase-shifting process. In the previous COACH [20,21], the correlation of H_{object} with the library of $H_{PSF}s$ yields the images at exactly the original axial locations. However, in the present configuration with the DL, the spatial information of the object, as well as the wavelength illumination, can be extracted. Hence, it is possible to acquire spatial, as well as spectral, information about the object using the 4D-COACH technique. In other words, the $H_{PSF}s$ of different wavelengths can be used to demultiplex the specific wavelength information from the object hologram, in addition to the spatial information.
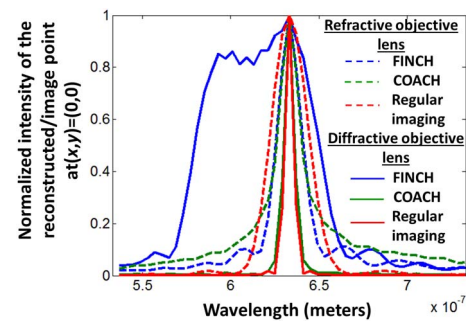
The wavelength sensitivity of the different systems FINCH, COACH, and regular imaging with a refractive lens and a DL was studied by simulating the beam propagation in the respective systems under identical conditions similar to the experimental setup. A detailed description of the $H_{PSF}s$ calculation is presented in [20,21]. The reference hologram H_{PSF} was recorded for $\lambda = 633$ nm, and it was correlated with $H_{PSF}s$ recorded for different wavelengths from 534 to 733 nm. The normalized intensity of the image at $(x, y) = (0, 0)$ is calculated for each imaging method. The plots of the point image intensity at $(x, y) = (0, 0)$ versus the wavelength of the source for COACH, FINCH, and regular imaging are plotted in Fig. 2. The graphs of COACH and regular imaging in Fig. 2 can be explained using the model of transmission of a Gaussian beam through a thin lens [27]. In the case of regular imaging with a refractive objective lens, there is only a single DL which is displayed on the SLM. The focal distance of this DL is $f = R\Omega/\lambda$, where R is the radius of the DL, and Ω is the smallest cycle of the DL. The differentiation of f with respect to λ, and the substitution of $\Omega = f\lambda/R$ yields the expression $\Delta f = (f\Delta\lambda/\lambda)$ for any change of the focal distance due to wavelength change $\Delta\lambda$. The width of the intensity curve $I(\lambda)$ near the focal point is obtained by comparing Δf to the width of the axial focus curve, given by [27], $\Delta z = 2\lambda f^2/\pi R^2$. Following this calculation, the width of the curve $I(\lambda)$ is $\Delta\lambda = (2\lambda^2 f/\pi R^2)$. When the diffractive objective lens replaces the refractive objective lens, the sensitivity of each DL to the wavelength is similar but the final curve $I(\lambda)$ is obtained as a product of two Lorenzians, each of which is contributed by one of the DL. A detailed calculation of the width of the product of two Lorenzians indicates that if the focal distance of the diffractive objective lens is about half of the focal distance of the other DL displayed on the SLM, the overall width of $I(\lambda)$ is 40% of the width with the refractive objective lens i.e., $\Delta\lambda \simeq 0.4(2\lambda^2 f/\pi R^2)$. In the configuration with DL as the objective lens, the wavelength sensitivity of COACH and regular imaging matched well. In the case with the diffractive objective lens, the wavelength sensitivity is found to be almost independent of the distance between the SLM and the sensor. Both phenomena are because the wavelength sensitivity is mainly dictated by the dispersion of the diffractive objective lens. In the case of FINCH, the wavelength resolution is similar to that of COACH in the case of the refractive objective, but it is well known [20,21] that the low axial resolution of FINCH prevents us from using FINCH as a 4D imaging system.
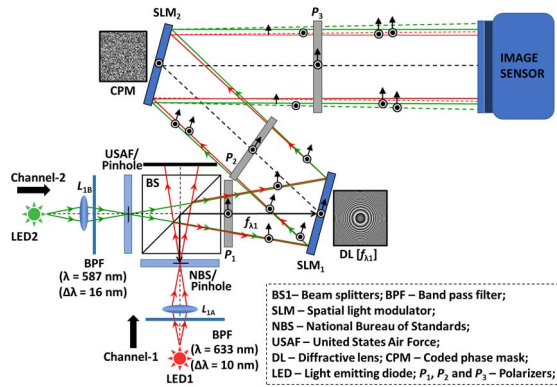
Fig. 3. Experimental setup of 4D COACH with two illumination channels for two wavelengths.

The correlation of the H_{object} with H_{PSF} yields the reconstructed image with disturbing background noise. In order to reduce the background noise, two noise reduction techniques were employed simultaneously, namely the phase-only filtering correlation technique and the averaging technique [21]. In the first technique, the phase-only filter of the Fourier transform of H_{PSF} filters the object hologram to improve the signal-to-noise ratio (SNR) and resolution. The SNR is improved further by recording the multiple object and PSF holograms using different CPMs and averaging the multiple complex reconstructed images [21].

The experimental verification of the 4D imaging was carried out using a digital holographic setup shown in Fig. 3. The experimental setup consists of two illumination channels corresponding to two light sources (LEDs) of different wavelengths namely, 635 nm (Thorlabs LED631E, 4 mW, $\lambda = 635$ nm, $\Delta\lambda = 10$ nm) and 565 nm (Thorlabs M565L3, 880 mW, $\lambda = 565$ nm, $\Delta\lambda = 104$ nm) in channel 1 and channel 2, respectively. Two bandpass filters ($\lambda = 633$ nm, $\Delta\lambda = 10$ nm) and ($\lambda = 587$ nm, $\Delta\lambda = 16$ nm) were used in channel 1 and 2, respectively, to narrow the bandwidth of the light sources. Two identical lenses, L_{1A} and L_{1B}, were used to critically illuminate two objects: element 8 lp/mm of the National Bureau of Standards (NBS) resolution chart and elements 10.1 and 11.3 lp/mm of group 3 of the United States Air Force (USAF) resolution chart respectively. The distance between the lenses L_{1A} and L_{1B} and the NBS and USAF objects, respectively, was 3 cm, while the diameter of the beam at the output of the lens was 0.4 cm. Hence, the numerical aperture NA of the illumination system was approximately 0.067. However, the NA of the system is governed by the location ($\approx f_{\lambda1}$ from the object) and the aperture ($D = 8$ mm) of SLM_1 which, in this case, is approximately 0.016. Therefore, the lateral resolutions (0.61 λ/NA) are about 24 and 22 μm, and the axial resolutions [$2\lambda/(NA)^2$] are about 5 and 4.6 mm for the red and green wavelengths, respectively.

The light diffracted by the two objects were combined using a beam splitter (BS) and passed through polarizer P_1 oriented along the active axis of a phase-only reflective SLM_1 (Holoeye PLUTO, 1920 × 1080 pixels, 8 μm pixel pitch, phase-only modulation) to enable full modulation of light. The SLM_1 is tilted to an angle of about 15° with respect to the optical axis. In SLM_1, a DL with a focal length $f(\lambda_1 = 633$ nm) of 25 cm is displayed. Hence, the focal length of the diffractive objective lens at channel 1 and channel 2 is $f_{\lambda1} = 25$ cm and $f_{\lambda2} = 27$ cm, respectively. The distance between the objects and the BS is

9 cm, while the distance between the BS and SLM_1 is 18 cm at both channels. The off-axis illumination of SLM_1 introduced aberrations into the system which were corrected using correction coefficients introduced in the phase profile of the DL. The tilted configuration can be avoided using an additional beam splitter, but will result in the loss of the optical power. An alternative way to implement the experiment without a tilted configuration is to replace the SLM by a fabricated blazed diffractive objective lens [28]. The light with two wavelengths diffracted by the DL is passed through a polarizer P_2 to orient the light at 45° with respect to the active axis of SLM_2 on which the CPM is displayed. Polarizer P_2 would not be necessary if SLM_1 would receive normal light incidence. The distance between SLM_1 and SLM_2 is 25 cm. The SLM_2 is tilted by an angle of about 15° with respect to the optical axis. Only half of the intensity of light with the two wavelengths is modulated by the CPM, while the remaining half propagates without any modulation. A third polarizer P_3 oriented at an angle of 45° with respect to the active axis of SLM_2 is mounted after the SLM_2 to create interference between the light modulated by the SLM_2 with the unmodulated light at the image sensor (Hamamatsu ORCA-Flash4.0 V2 Digital CMOS, 2048 × 2048 pixels, 6.5 μm pixel pitch, monochrome). The distance between SLM_2 and the image sensor is $z_h = 43$ cm. For the above optics configuration, the wavelength resolution is about 6 nm (FWHM).

The experiment was carried out by recording $H_{PSF}s$ using a pinhole with a diameter of 50 μm for different axial locations and for the two wavelengths, each one in its turn, by blocking the other channel. Similarly, $H_{object}s$ were recorded. The complex H_{object} and $H_{PSF}s$ were synthesized by superposition of the recorded raw holograms using the phase-shifting procedure [13,14]. A phase-only filter computed from the spatial spectrum of H_{PSF} is used in the reconstruction process by the 2D spatial correlation. The averaging technique was implemented to reduce the noise further using 20 different CPMs. The thickness of the multiplane object can be adjusted by varying the location of the object (NBS or USAF) in one of the channels while keeping the location of the object in the other channel constant. Different cases of the multiplane objects are considered. In the first case, a single plane object is constructed by placing the NBS resolution chart illuminated by LED ($\lambda = 635$ nm) and a USAF resolution chart illuminated by LED ($\lambda = 587$ nm) at the same distance from the SLM_1 to study the wavelength sensitivity of the system. The $H_{PSF}s$ were also recorded exactly at the same locations and ±1 cm from the location in the two channels illuminated by the two different wavelengths. The correlation of the $H_{PSF}s$ with the H_{object} extracted the specific information of the wavelength illumination, as shown in Fig. 4. The H_{object}, when correlated with the processed H_{PSF} recorded with red light reconstructed only that part of the object plane illuminated by the red light, while the other part illuminated by the green light is defocused and vice versa. When the H_{object} was reconstructed using the processed $H_{PSF}s$ recorded at ±1 cm from the object plane, the object plane information was defocused.

The experiment was repeated by placing the NBS and USAF objects separated by a distance of 1 cm with respect to the SLM_1 and recording the hologram. The reconstruction was carried out using $H_{PSF}s$ recorded at the corresponding locations of the NBS and USAF objects and with respective wavelengths, as shown in Fig. 5. The experiment was carried out for FINCH
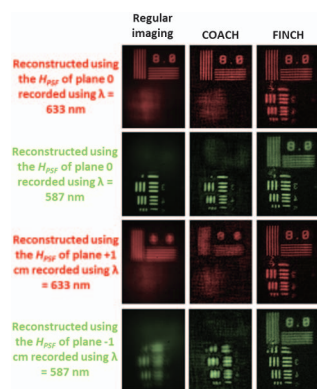
Fig. 4. Experimental comparison results of regular imaging, COACH, and FINCH holograms recorded by placing the NBS and USAF objects at a same distance from SLM$_1$. (The colors are given artificially for better understanding.)

using two DLs of focal lengths 25 cm and 20 cm displayed on SLM$_1$ and SLM$_2$, respectively. This setup achieves perfect overlap between the two interfering waves at the sensor plane [16]. In the case of regular imaging, the imaging was carried out using two DLs of focal lengths 25 cm and 40 cm displayed on SLM$_1$ and SLM$_2$, respectively. The focal distances were adjusted for imaging the other planes. It can be noted in Figs. 4 and 5 that the performance of COACH is similar to that of regular imaging, as expected from the similarity of both imaging methods with respect to their spatial and spectral resolutions. The H_{PSF} library of COACH can effectively demultiplex the spectral specific information from the hologram. In the case of FINCH, the lower axial resolution prevents such an extraction.

In conclusion, we have proposed and demonstrated a 4D COACH system for recording and reconstructing 4D information of objects. The optical configuration of COACH has been advanced using a DL to enhance its wavelength resolution, and this enhancement is successfully exploited for resolving wavelengths. Although the process of creating the library of $H_{PSF}(\lambda, z)$ for different axial distances and wavelengths seems time-consuming, this process is done only once, off-line, as a part of training the system. Once the training phase is completed, the process of target acquisitions is not different form
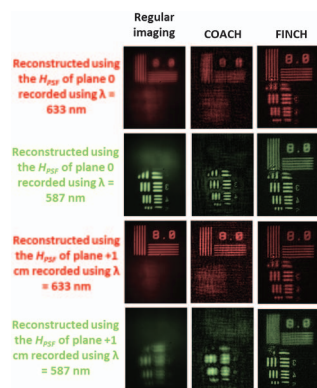
other digital hologram recorders such as FINCH. The training process can be speeded up using automatic computer-controlled translational stages. At least conceptually, a further speeding up of the process can be achieved by synthesizing the library of $H_{PSF}(\lambda, z)$ digitally in the computer. Such a computation might succeed by simulating the beam propagation along the optical system with the accurate experimental parameters and taking into account the entire system aberrations. The low intensity problem arising while recording H_{PSF}s with small pinholes can be solved by the use of higher-power light sources. The 4D COACH holographic technique is demonstrated for two wavelengths, and it can be extended to polychromatic light just by recording additional H_{PSF}s for different wavelengths. Although the efficiency of the DL is decreased in case the spectral bandwidth of the incident light is wider than the DL bandwidth, the efficiency can be optimized by compensation (at least theoretically) with a proper curve of the refraction index versus the wavelength.

REFERENCES

1. D. Gabor, Nature **161**, 777 (1948).
2. G. Tricoles, Appl. Opt. **26**, 4351 (1987).
3. G. Indebetouw, Y. Tada, J. Rosen, and G. Brooker, Appl. Opt. **46**, 993 (2007).
4. F. Dubois, L. Joannes, and J.-C. Legros, Appl. Opt. **38**, 7085 (1999).
5. C. J. Mann, L. Yu, C.-M. Lo, and M. K. Kim, Opt. Express **13**, 8693 (2005).
6. G. Indebetouw and P. Klysubun, Opt. Lett. **25**, 212 (2000).
7. W. Xu, M. H. Jericho, H. J. Kreuzer, and I. A. Meinertzhagen, Opt. Lett. **28**, 164 (2003).
8. Q. Lü, Y. Chen, R. Yuan, B. Ge, Y. Gao, and Y. Zhang, Appl. Opt. **48**, 7000 (2009).
9. J. Garcia-Sucerquia, W. Xu, S. K. Jericho, M. H. Jericho, and H. J. Kreuzer, Optik **114**, 419 (2007).
10. X. Yu, J. Hong, C. Liu, M. Cross, D. T. Haynie, and M. K. Kim, J. Biomed. Opt. **19**, 045001 (2014).
11. X. Shi, B. Yuan, W. Zhu, E. Liang, X. Liu, and F. Ma, Proc. SPIE **9271**, 92710W (2014).
12. D. Donnarumma, A. Brodoline, D. Alexandre, and M. Gross, Opt. Express **24**, 26887 (2016).
13. J. Rosen and G. Brooker, Opt. Lett. **32**, 912 (2007).
14. J. Rosen and G. Brooker, Nat. Photonics **2**, 190 (2008).
15. P. Bouchal, J. Kapitán, R. Chmelík, and Z. Bouchal, Opt. Express **19**, 15603 (2011).
16. J. Rosen, N. Siegel, and G. Brooker, Opt. Express **19**, 26249 (2011).
17. R. Kelner, J. Rosen, and G. Brooker, Opt. Express **21**, 20131 (2013).
18. J. Rosen and R. Kelner, Opt. Express **22**, 29048 (2014).
19. X. Lai, S. Xiao, Y. Guo, X. Lv, and S. Zeng, Opt. Express **23**, 31408 (2015).
20. A. Vijayakumar, Y. Kashter, R. Kelner, and J. Rosen, Opt. Express **24**, 12430 (2016).
21. A. Vijayakumar, Y. Kashter, R. Kelner, and J. Rosen, Appl. Opt. (to be published).
22. C.-I. Chang, *Hyperspectral Imaging: Techniques for Spectral Detection and Classification* (Plenum, 2003), pp. 1–4.
23. J. B. Pawley, *Handbook of Biological and Confocal Microscopy*, 1st ed. (Plenum, 1990), pp. 1–4.
24. R. W. Gerchberg and W. O. Saxton, Optik **34**, 275 (1971).
25. R. W. Gerchberg and W. O. Saxton, Optik **35**, 227 (1972).
26. G. Brooker, N. Siegel, V. Wang, and J. Rosen, Opt. Express **19**, 5047 (2011).
27. B. E. A. Saleh and M. C. Teich, *Fundamentals of Photonics* (Wiley, 2007).
28. T. Fujita, H. Nishihara, and J. Koyama, Opt. Lett. **7**, 578 (1982).

Fig. 5. Experimental comparison results of regular imaging, COACH, and FINCH holograms recorded by placing the NBS and USAF objects separated by a distance of 1 cm with respect to SLM$_1$. (The colors are given artificially for better understanding.)